Structure−Property Relationship for Two-Photon Absorbing Multiporphyrins: Supramolecular Assembly of Highly-Conjugated Multiporphyrinic Ladders and Prisms

Shanmugam Easwaramoorthi,[‡] So Young Jang,[‡] Zin Seok Yoon,[‡] Jong Min Lim,[‡] Cheng-Wei Lee,[§] Chi-Lun Mai,[§] Yen-Chun Liu,[§] Chen-Yu Yeh,*[,§] Josh Vura-Weis,[†] Michael R. Wasielewski,*[,†] and Dongho Kim*[,‡]

Department of Chemistry, Yonsei University, Seoul 120-749, Korea, Department of Chemistry, and Centre for Nanoscience and Nanotechnology, National Chung Hsing University, Taichung, Taiwan, and Department of Chemistry, Argonne-Northwestern Solar Energy Research (ANSER) Center, and International Institute for Nanotechnology, Northwestern University, Evanston, Illinois 60208-31

Received: February 25, 2008; Revised Manuscript Received: May 13, 2008

Two-photon absorption (TPA) phenomena of a series of single-strand as well as supramolecular self-assembled ladders and prisms of highly conjugated ethyne bridged multiporphyrin dimer, trimer, and star shaped pentamer have been investigated. The ligand mediated self-assembled supramolecular structures were characterized by UV−visible spectroscopy and small- and wide-angle X-ray scattering (SAXS/WAXS) analysis. The TPA cross section values of multiporphyrins increase nonlinearly from ∼100 to ∼18000 GM with an increased number of porphyrin units and elongated π-conjugation length by virtue of charge transfer and excited-state cumulenic configurations. The observed opposite TPA behavior between their supramolecular ladder and prism configurations necessitates the importance of interstrand interactions between the multiporphyrinic units and the overall shape of the assembly. Furthermore, the diminished TPA cross section of the pentamer, despite the increased π-conjugation resulting from duplex formation suggests that destabilizing the essential functional configurations at the cost of elongation of π-delocalization pathway must cause unfavorable effects. We have also shown that one- and two-photon allowed energy-levels of linear multiporphyrins are nearly isoenergetic and the latter transition originates exclusively from the extent of π-delocalization within the molecule. The identical TPA maximum position of the trimer and pentamer indicates that the TPA of the pentamer arises only from its basic trimer unit in spite of its extended two-dimensional π-conjugation pathway involving five porphyrinic units.

Introduction

Molecules with strong two-photon absorption (TPA) properties find potential applications ranging from photodynamic therapy to micro- and nanofabrication, three-dimensional (3D) fluorescence microscopy, optical power limiting and high-density optical storage.[1] Inspired by the fruitful applications of TPA, much attention has been paid to the design and synthesis of new molecules with large two-photon absorptivities.[2] As a consequence, molecules having donor−acceptor configuration with intervening π-conjugation (D−π−A) are proposed to be better two-photon absorbers.[3] In this regard porphyrin molecules deserve particular attention due to their highly delocalized π-conjugation pathway, ease of fuctionalization at the β and meso positions and complexation ability with a range of metal ions to tailor the molecules to achieve desired properties. However, the TPA cross sections, $\sigma^{(2)}$ of a majority of regular porphyrins do not exceed 1−10 GM (1 GM = 10^{-50} cm^4 s photon^{-1}) in the biologically important range of near-IR region.[4] On the other hand, multiporphyrins, porphyrins with donor/acceptor substituents and expanded porphryins exhibit enhanced TPA cross section values.[5] We have recently reported the TPA properties of directly linked meso−meso multiporphyrins and the influence of the dihedral angle between the porphyrin units that is in fact directly correlated to the π-electron delocalization efficiency throughout the chain.[6]

The effective π-conjugation between the porphyrins can be expanded by introducing alkyne links that permit the coplanar orientation of the molecules.[7] Still, porphyrin macrocyles deviate from planarity and such deviations are considered to be detrimental to the effective π-conjugation.[8] It is well-known that the formation of supramolecular assemblies is an effective way of arranging the large irregularly shaped molecules in an orderly manner.[9] Anderson and his co-workers[10] have utilized the ligand mediated supramolecular assembly to enforce a planar configuration of the butadiyne linked porphyrin oligomers. It was found that the TPA cross section of a double-strand supramolecular structure is dramatically enhanced as a result of increased π-conjugation efficiency. In a similar fashion, Kobuke and his co-workers[11] showed that slipped cofacial arrangement by complementary coordination of imidazolyl nitrogen to the central zinc metal of porphyrin can effectively increase the TPA cross sections. The self-assembly of butadiyne bridged multiporphyrins is susceptible to adopt any forms with respect to ligands, for example it forms supramolecular prism with tritopic ligands, but detailed studies are yet to appear.[12]

In this work, we have studied the TPA properties of highly π-conjugated ethyne bridged porphyrins in single-strand, multiplex and prism configurations. Ethyne linkage between the porphyrin units facilitate effective π-electron delocalization and

* Corresponding authors. E-mail: D.K., dongho@yonsei.ac.kr; C.-Y.Y., cyyeh@dragon.nchu.edu.tw; M.R.W., m-wasielewski@orthwestern.edu.
‡ Yonsei University.
§ National Chung Hsing University.
† Northwestern University.

10.1021/jp801626s CCC: $40.75
Published on Web 06/28/2008

ensure the planarity of the molecule.[13] We have employed ditopic and tritopic donor ligands to make a multiporphyrin ladder and prism, respectively. As the interaction between the porphyrin units is affected by its orientation and distance between the individual components in the self-assembled structure, it is important to have a basic knowledge about the relationship between the shape of supermolecule and its nonlinear optical properties. We have also controlled the planarity of the sterically crowded multiporphyrin system and its π-conjugation efficiency by varying the molecular length of the ligand, which helps to understand the intermolecular interactions in supramolecular multiplex. In this report, particular attention is paid to the structure−property relationships between two-photon absorbing multiporphyrins in ladder, multiplex and prism structures.

Experimental Section

Sample Preparation. Synthesis of highly conjugated ethyne bridged multiporphyrin was reported previously.[13a] All the spectral and titration experiments were carried out in dichloromethane (Aldrich, Spectrophotometric grade) solvent. 4,4′-Bipyridyl, 1,4-diazabicyclo[2.2.2]octane, 1,2-di(4-pyridyl)ethylene and pyridine are purchased from Aldrich and was used without further purification. 1,3,5-tris(pyridin-4-ylethynyl)benzene was synthesized on the basis of the literature procedure.[14] All spectrophotometric titration studies were carried out in 1−3 μM concentration range, the concentration of supramolecular assemblies for TPA studies are in the range of about 0.05−0.06 mM. Structural determinations of supramolecular complexes by SAXS were carried out in solution using toluene or methylcylclohexane as a solvent. In both cases the formation of supramolecular multiporphyrin structures was understood from the respective spectral changes during the formation of the supramolecular complex and its dissociation at excess ligand concentration.

Steady-State Absorption and Fluorescence. Absorption spectra were obtained with a Varian model Cary 5000 UV−vis−NIR spectrophotometer, and steady-state fluorescence spectra were measured by a Hitachi model F-2500 or 7000 fluorometer at room temperature.

SAXS Measurements. X-ray scattering measurements were carried out at beam lines 12-BM and 12-ID at the Advanced Photon Source (APS), Argonne National Laboratory. A quartz capillary (0.2 mm diameter) was used as sample container. All samples were filtered prior to measurement (0.2 μm PTFE, VWR). The X-ray scattering from ~ 0.03 Å$^{-1} < q < 1.0$ Å^{-1} was collected using a two-dimensional mosaic CCD detector.[15] The scattering intensity was averaged over 5−10 measurements and subtracted from a solvent blank. Models of the self-assembled structures were optimized using the MM+ force field in the program HyperChem[16] and fitting the simulated scattering of the MM+ model were done by the reported method.[17]

TCSPC Measurements. Time-correlated single photon counting (TCSPC) system was used for the spontaneous fluorescence decay measurement. The system consisted of a cavity-dumped Kerr lens mode-locked Ti:sapphire laser pumped by a continuous wave (CW) Nd:YVO_4 laser (Coherent, Verdi). The full width at half-maximum (fwhm) of the instrument response function (IRF) obtained by a dilute solution of coffee cream was typically 70 ps in our TCSPC system. The fluorescence decays were measured with magic angle (54.7°) fluorescence polarization, and the number of fluorescence photons per unit time, detected by photomultiplier tube, was always maintained to <1% of the repetition rate of the excitation pulses, to prevent pile-up distortion in the decay profiles. Time-resolved fluorescence anisotropy decays were obtained by changing the detection polarization on the fluorescence path parallel or perpendicular to the polarization of the excitation light. The anisotropy decays then were calculated as follows:

$$r(t) = \frac{I(t)_{vv} - GI(t)_{VH}}{I(t)_{vv} + 2GI(t)_{VH}}$$

where $I(t)_{VV}$ (or $I(t)_{VH}$) is the fluorescence decay when the excitation light is vertically polarized and only the vertically (or horizontally) polarized portion of fluorescence is detected, denoting that the first and second subscripts represent excitation and detection polarization, respectively. The factor G is defined by $I(t)_{VV}/I(t)_{VH}$, which is equal to the ratio of the sensitivities of the detection system for vertically and horizontally polarized light. The G factor of our detection system was 1.37.

Measurement of Two-Photon Absorption Cross-Section ($\sigma^{(2)}$). The TPA experiments were performed using the open-aperture Z-scan method with 130 fs pulses from an optical parametric amplifier (Light Conversion, TOPAS) operating at a 5 kHz repetition rate using a Ti:sapphire regenerative amplifier system (Spectra-Physics, Hurricane). The laser beam was divided into two parts. One was monitored by a Ge/PN photodiode (New Focus) as an intensity reference, and the other was used for the transmittance studies. After passing through an $f = 10$ cm lens, the laser beam was focused and passed through a quartz cell. The position of the sample cell could be varied along the laser-beam direction (z-axis), so the local power density within the sample cell could be changed under a constant laser power level. The thickness of the cell is 1 mm. The transmitted laser beam from the sample cell was then probed using the same photodiode as used for reference monitoring. The on-axis peak intensity of the incident pulses at the focal point, I_0, ranged from 40 to 60 GW/cm. Assuming a Gaussian beam profile, the nonlinear absorption coefficient β can be obtained by curve fitting to the observed open aperture traces with the following equation:

$$T(z) = 1 - \frac{\beta I_0 (1 - e^{-a_0 l})}{2\alpha_0 (1 + (z/z_0)^2)}$$

where α_0 is the linear absorption coefficient, l the sample length, and z_0 the diffraction length of the incident beam. After obtaining the nonlinear absorption coefficient β, the TPA cross-section $\sigma^{(2)}$ (in units of 1 GM = 10^{-50} cm^4 s/photon/molecule) of a single solute molecule sample can be determined by using the following relationship:

$$\beta = \frac{\sigma^{(2)}(N_A d \times 10^{-3})}{h\nu}$$

where N_A is the Avogadro constant, d the concentration of the TPA compound in solution, h is Planck's constant, and ν is the frequency of the incident laser beam. So as to satisfy the condition of $\alpha_0 l \ll 1$, which allows the pure TPA $\sigma^{(2)}$ values to be determined using a simulation procedure, the TPA cross-section of AF-50 was measured as a reference compound; this control was found to exhibits a TPA value of 50 GM at 800 nm.

Results and Discussion

Spectral Properties of Multiporphyrins. We have synthesized ethyne linked multiporphyrin dimer (**1**), trimer (**2**) and star shaped pentamer (**3**) represented in Chart 1[13a]

CHART 1

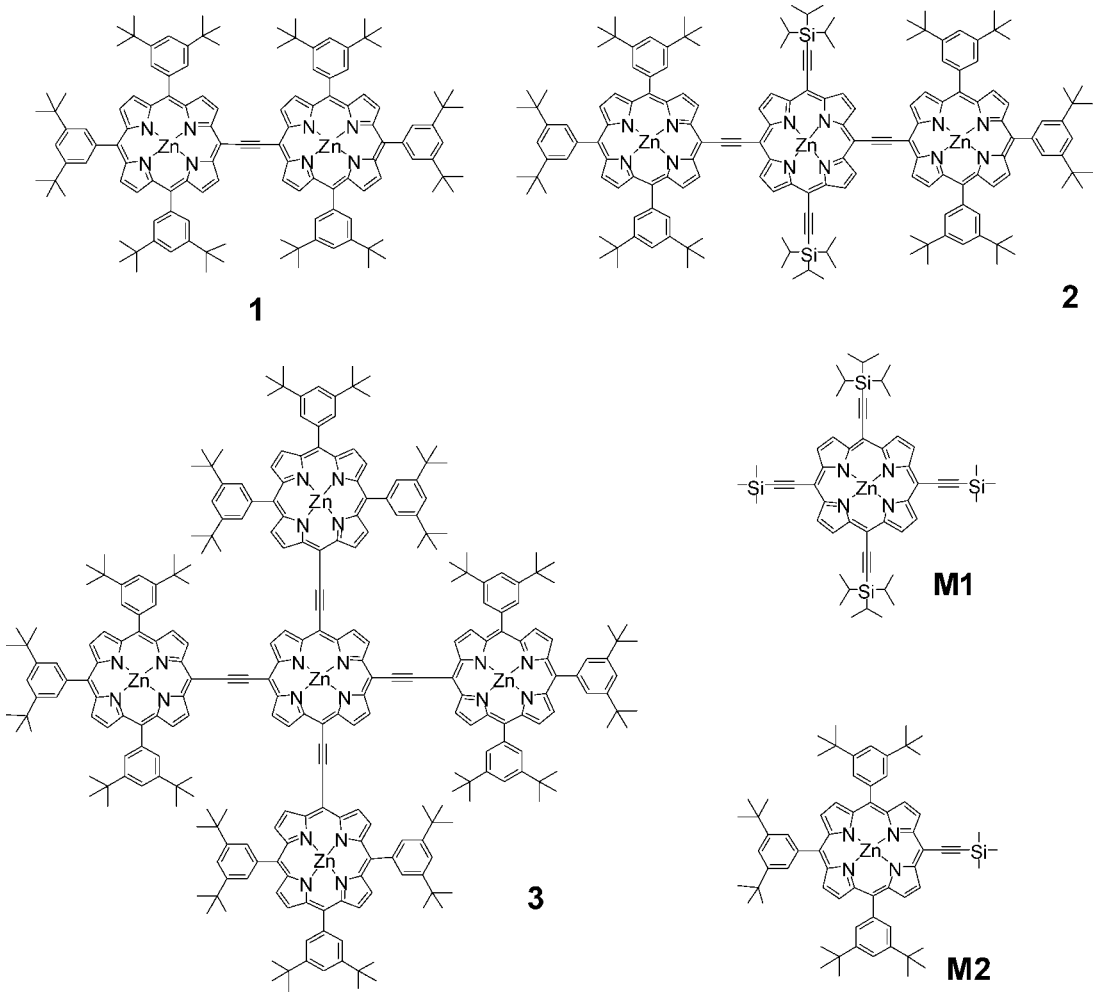

TABLE 1: Photophysical and Two-Photon Absorption Properties of Conjugated Multiporphyrins in Single-Strand and Self-Assembled Form

molecule	τ_{fl}, ns	Φ, ns	$\sigma^{(2)}$/GM (per porphyrin unit)	absorption maximum, nm: two photon	absorption maximum, nm: one photon
M1	2.53	0.31			
M2	2.14	0.35			
1	1.11	1.28	4700 ± 500 (2300)	1380	696
1Py$_{(excess)}$	1.12	1.35	5000 ± 500 (2500)	1420	726
1$_2$**Bpy**$_2$	1.15	3.4	4400 ± 500 (2200)	1420	725
1$_3$**Tpy**$_2$	1.10	4.7	2900 ± 500 (1400)	1380	729
2	1.27	2.24	14500 ± 1000 (4000)	1500	761
2Py$_{(excess)}$	1.08		15400 ± 1000 (5100)	1500	799
2$_2$**Bpy**$_3$	1.03		21600 ± 1000 (7200)	1520	804
3$_3$**Tpy**$_3$	1.11		9600 ± 1000 (3200)	1460	813
3	1.58	4.95	18700 ± 1000 (3700)	1500	787
3Py$_{(excess)}$	1.06		18500 ± 1000 (3700)	1540	832
3$_2$**Bpy**$_5$	1.03		13400 ± 1000 (2600)	1500	870
3$_2$**Epy**$_5$	1.07		15500 ± 1000 (3000)	1580	856
3$_2$**DABCO**$_5$	1.34		13200 ± 1000 (2600)	1520	839
3$_3$**DABCO**$_{10}$	1.48		14400 ± 1000 (2800)	1560	825

The spectral properties of multiporphyrins are discussed in detail in our earlier report.[13a] Briefly, the Q-absorption band and fluorescence maximum are red-shifted progressively while going from monomer to pentamer (SI, Figure S1) which could be explained by the decreased HOMO−LUMO energy gap due to the extensive π-electron delocalization between the neighboring porphyrin units. Subsequently, the fluorescence lifetime (τ_{fl}) of **1** is diminished to nearly half-with respect to its basic monomer unit **M2** (τ_{fl} = 2.14 ns) in accordance with the accelerated S_1-S_0 internal conversion caused by the reduced S_0-S_1 energy gap (Table 1). Despite the increased π-conjugation length, the longer fluorescence lifetimes observed for multiporphyrins **2** and **3** relative to **1** are attributed to the central zinc porphyrin with peripheral ethyne substituents, which has significantly lower energy than the remaining units, acting as an excitation energy acceptor unit upon photoexcitation. Thus the overall fluorescence lifetimes of **2** and **3** are mainly determined by the central zinc porphyrin which gives rise to

SCHEME 1

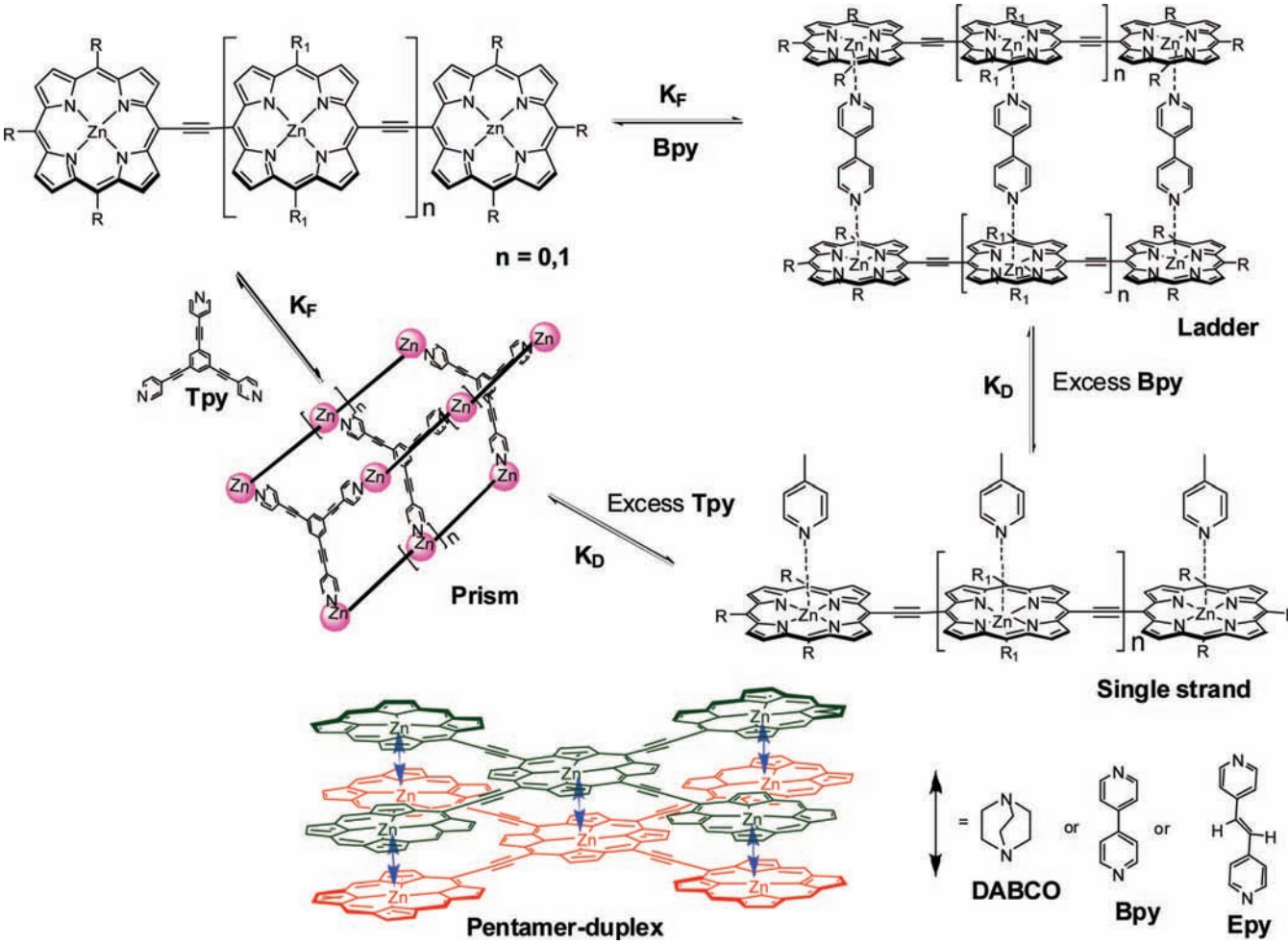

slightly different fluorescence decay with respect to terminal zinc porphyrin units. The considerably longer fluorescence lifetime of **3** compared with **2** is presumably due to more restricted environment of the central zinc porphyrin unit in pentamer.

Supramolecular Complexation. The reversible coordination of donor ligands such as ditopic 4,4′-bipyridyl (**Bpy**) and tritopic 1,3,5-tris(pyridin-4-ylethynyl)benzene (**Tpy**) with multiporphyrins **1** and **2** leads to the formation of ladder and prism shaped self-assembled structures, respectively, as illustrated in Scheme 1.

The binding of the pyridyl moiety to the central zinc metal of porphyrin results in red-shifted B- and Q-bands with an appearance of isosbestic points in a series of absorption spectra in the titration experiment as shown in Figure 1, which allows the unequivocal assignment of only two defined species viz. the coexistence of uncoordinated and ladder shaped multiporphyrins in solution.

The observed binding stoichiometry of multiporphyrin complexes identified from the Job's continuous variation method confirms the formation of $\mathbf{1}_2\mathbf{Bpy}_2$, $\mathbf{2}_2\mathbf{Bpy}_3$ ladders and $\mathbf{1}_3\mathbf{Tpy}_2$, $\mathbf{2}_3\mathbf{Tpy}_3$ prisms, although excess ligand concentration causes additional spectral changes, implying that further ligation induces the destruction of the supramolecular assembly (SI, Figure S2). The stability constant (K_f) values of the supramolecular complex were determined by the multivariate global analysis method using Specfit software[18] with three colored species model, viz., uncoordinated multiporphyrin, self-assembly and open complex (see SI for the stability constants). The higher stability constants and sustainability of supramolecular structures in the presence of excess ligand concentration viewed from the speciation profile generated by the Specfit program suggest that longer ladders and prisms are more stable than shorter ones (SI, Figure S3).

The supramolecular complexation of star-shaped pentamer **3** with **Bpy** resulting in the formation of the $\mathbf{3}_2\mathbf{Bpy}_5$ duplex goes through a nonisosbestic pathway, indicating the involvement of multiple equilibrium reaction steps (SI, Figure S4). As

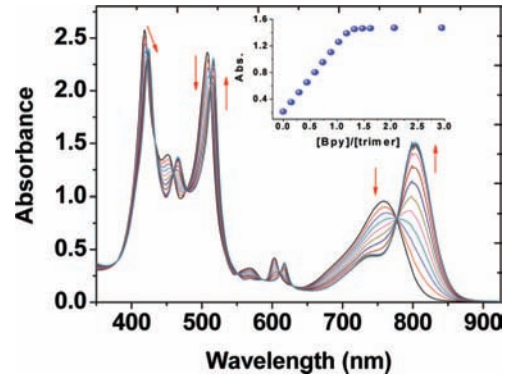

Figure 1. UV−visible spectrophotometric titration of trimer **2** with **Bpy** for ladder formation (0, 0.15, 0.3, 0.44, 0.59, 0.74, 0.88, 1.03, 1.18, 1.33, 1.47, 1.62, 2.06, 2.95, 4.4,6.9, 9.3, and 14 equiv). Inset: plot of molar ratio vs absorbance at 813 nm.

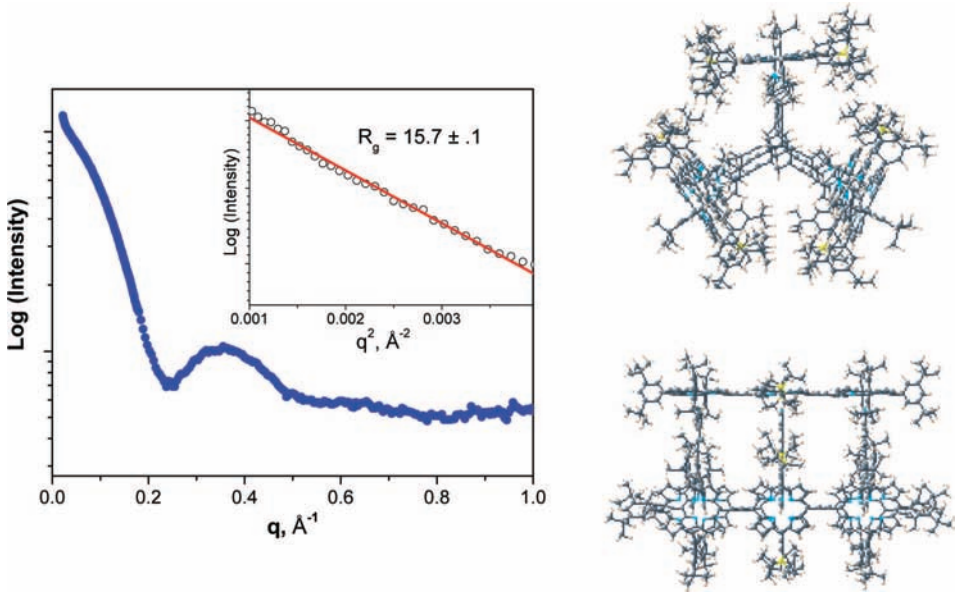

Figure 2. X-ray scattering data for trimer prism $\mathbf{2_3Tpy_3}$ in toluene, with MM+ optimizedstructure. Inset: low-q region with Guinier fit.

a result of complexation, the intensity of B-band is decreased accompanied by a significant enhancement of Q-band with a large red-shift from 787 to 870 nm (ca. 83 nm) for $\mathbf{3_2Bpy_5}$ compared to $\mathbf{3Py_{(excess)}}$ (ca. 46 nm) indicating the occurrence of significant structural changes in the pentamer. The semiempirical PM3 level energy minimized structure of **3** (SI, Scheme S1) demonstrates that the peripheral porphyrin moieties adopt a notable dihedral angle with respect to the central porphyrin macrocyle due to steric interactions between the meso-t-butyl substituted phenyl groups. Thus the supramolecular complex formation forces the constituent porphyrin units to be coplanar by restricting free rotation around the C−C alkyne bond, which in turn increases the interporphyrin π-conjugation pathway and explains the further red-shifted Q-band.[19] This interpretation is further supported by the small- and wide-angle X-ray scattering studies (vide supra).

Because it is possible to control the degree of planarity of **3** by changing the molecular length of the ligand, we have selected 1,2-di(4-pyridyl)ethylene (**Epy**) and 1,4-diazabicyclo[2.2.2]octane (**DABCO**) with the molecular lengths (the distance between the nitrogen atoms) of 9.4 and ∼3 Å, which are longer and shorter, respectively, than bipyridyl (∼7 Å). Although reversible coordination of **Epy** with **3** is reminiscent of that for **Bpy** to form $\mathbf{3_2Epy_5}$, the binding of **DABCO** with **3** proceeds through isosbestic and nonisosbestic pathways toward the formation of $\mathbf{3_2DABCO_5}$ (SI, Figure S4). Interestingly, the continuous addition of **DABCO** gives rise to a blue-shifted Q-band with the appearance of isosbestic point (SI, Figure S4) and the analysis of the titration data indicates the stoichiometric formation of 2:5 and 3:10 complexes in which the latter exhibits higher stability (SI, Figure S3). Among the pentamer duplexes, the stability constant of $\mathbf{3_2Bpy_5}$ is higher than those of $\mathbf{3_2Epy_5}$ and $\mathbf{3_2DABCO_5}$ by several orders of magnitude (SI, Table S1), because the interporphyrin distance between the pentamers in $\mathbf{3_2DABCO_5}$ becomes shorter due to the shorter length of the ligand; the steric interaction between the pentamers destabilizes the supramolecular structures. The putative $\mathbf{3_3DABCO_{10}}$ complex may show many possible isomeric structures, in which the isomer with 5 out of 10 **DABCO** units is sandwiched between the two pentameric porphyrin units whereas the remaining ones in the monocoordinated form are expected to show higher stability than the others (SI, Scheme S2).

The relatively high oscillator strength of low-energy Q-band noted for pentamer complexes with **Bpy** followed by **Epy** and **DABCO** implies that the degree of planarity and the extent of porphyrin−porphyrin electronic coupling go parallel with each other. This feature indicates that **Bpy** has the appropriate molecular length to make **3** in planar or nearly planar form, whereas the molecular length of **Epy** is sufficiently large enough to bind with pentamer **3** without much change in its original structure. The feasibility of H-aggregated structures cannot be excluded in the case of **DABCO** due to its smaller molecular size; the blue-shifted absorption spectrum is consistent with an increased aggregation number from 2 to 3 pentamer moieties.

Small- and Wide Angle X-Ray Scattering. Small- and wide-angle X-ray scattering (SAXS/WAXS) of the $\mathbf{2_2Bpy_3}$, $\mathbf{2_3Tpy_3}$, and $\mathbf{3_2Bpy_5}$ complexes adds support to the structures inferred from the UV−vis spectrophotometric titration.

The scattering intensity of 10^{-5} M $\mathbf{2_3Tpy_3}$ in toluene as a function of scattering vector q ($q = [(4\pi/\lambda) \sin \theta]$), is shown in Figure 2, along with the MM+ optimized structure. The low-q region ($q < 0.08$) was fitted using a least-squares method to the Guinier relationship $I(q) = I(0) \exp(-q^2R_g^2/3)$,[20] where $I(0)$ is the forward scattering amplitude and R_g is the radius of gyration, which is the root-mean-square distance of the electron density from the center of mass. An R_g of 15.7 Å was obtained from the experimental scattering data, which is in excellent agreement with the value of 15.5 Å obtained from fitting the simulated scattering of the MM+ model. In contrast, MM+ models of monomer **2** and $\mathbf{2_2Tpy_3}$ (the prism structure with one side removed) yield R_g values of 11.6 and 14.5 Å, respectively.

To further confirm the structure, a Fourier transform was performed on both the experimental data and simulated scattering from the models using the program GNOM,[21] as shown in Figure 3. The experimental PDF matches best with the simulated $\mathbf{2_3Tpy_3}$ PDF, with a peak around 20 Å. The simulated PDF of monomer **2** peaks at 13 Å, and that of the $\mathbf{2_2Tpy_3}$ test structure is several angstroms broader than the experimental result. It should be noted that the PDF analysis of the model complexes was performed on a q range of 0.001−2.7 Å^{-1}, leading to a greater degree of fine structure in the simulated than the experimental curves.

Guinier fits of the low-q regions of $\mathbf{2_2Bpy_3}$, and $\mathbf{3_2Bpy_5}$ also gave strong support to their structural assignments (SI, Figures

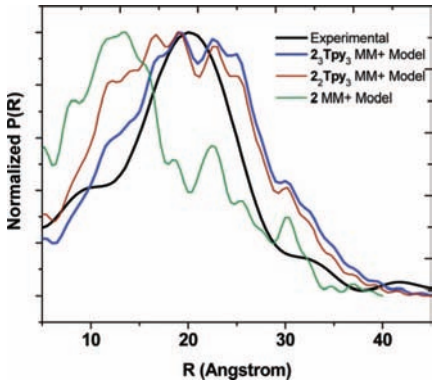

Figure 3. Experimental and Simulated PDF for trimer prism $\mathbf{2_3Tpy_3}$.

S5−8). $\mathbf{2_2Bpy_3}$ yielded an R_g of 12.6 Å, in good agreement with the 12.8 Å value of the MM+ model. A test structure in which one of the sides of the ladder is shifted by one porphyrin unit gave $R_g = 13.5$ Å, significantly larger than the observed value. The experimental and model Guinier fits of $\mathbf{3_2Bpy_5}$ gave R_g values of 13.7 and 14.0 Å, respectively, compared to 13.1 Å for the monomer model. PDF analysis of $\mathbf{2_2Bpy_3}$ and $\mathbf{3_2Bpy_5}$ (SI, Figures S5 and S6) is consistent with their respective MM+ models, though for these systems the PDFs of several test models are similar to those of the proposed structures, and the experimental data lack the resolution to distinguish them. The higher scattering efficiency of chlorine in dichloromethane restricts its usage in SAXS experiments. It is noteworthy that the degree of planarity of $\mathbf{3_2Bpy_5}$ is greatly influenced by the nature of the solvent. On the basis of the Q-band maximum and its oscillator strength ($\lambda_{max} = 840$ (toluene) and 870 nm (dichloromethane)), it is expected that **3** is more planar in dichloromethane; hence the photophysical properties of **3** reported here are obtained from a more planar structure than that determined by SAXS.

Photophysical Studies of Supramolecular Complexes. The significant differences in the UV−visible absorption spectra of the porphyrin ladder, prism and pyridine coordinated single-strand system, in spite of their indistinguishable local coordination environment, demonstrate that there are indeed interstrand interactions between the multiporphyrin units (SI, Figure S9). For example, the Q-band maximum of multiporphyrins is red-shifted in the prism configuration besides higher oscillator strength than the ladder form in which weak interstrand exciton coupling between the face-to-face porphyrins must cause a slight blue-shift in the absorption spectrum.[22] In contrast; the fluorescence spectra of self-assembled structures do not show any remarkable differences with respect to single-strand. Subsequently, the star shaped pentamer **3** shows ligand length dependent spectral features as it controls the overall structure of the self-assembly. The fluorescence maximum is red-shifted to the near IR region in the order $\mathbf{3_2Bpy_5}$ (908 nm), $\mathbf{3_2Epy_5}$ (889 nm), $\mathbf{3_2DABCO_5}$ (884 nm) $\mathbf{3_{10}DABCO_{10}}$ (875 nm) and single-strand $\mathbf{3Py_5}$ (842 nm), consistent with the increased electronic coupling between the porphyrin units by means of the enhanced degree of planarity in the assemblies. The fluorescence lifetimes for the self-assembled porphyrin structures suggest that there is no obvious difference between single-strand and self-assembled structures except for the putative $\mathbf{3_5DABCO_{10}}$ multiplex (Table 1). We have attempted to find out the rotational diffusion time (Φ) of the self-assembly from the fluorescence anisotropy decay to see the increase in molecular size through supramolecular complexation. Consequently, the rotational diffusion time of dimer increases in the order single-strand, ladder and prism, consistent with an increase in molecular size. However, we are unable to determine the rotational diffusion times of trimer and pentamer supramolecular assemblies due to their much larger molecular sizes.

Two-Photon Absorption Properties. Two-photon absorption (TPA) cross sections of various multiporphyrin assemblies were determined by using an open aperture Z-scan method. Though the TPA cross section values of monomers **M1** and **M2** were found to be less than ∼100 GM, multiporphyrin assemblies show intensely amplified TPA values up to ∼18000 GM with an increased number of porphyrin units going from dimer to pentamer (Table 1). Strong enhancement in TPA values as a function of the number of porphyrin units seems to originate from the larger polarizability due to effective π-delocalization along the elongated π-conjugation pathway. Although **3** shows a higher TPA cross section than **2,** it is not in accordance with the increased number of constituent porphyrin macrocyles, in fact the TPA cross section per porphyrin unit of **3** is an order of magnitude smaller than that of **2**. The higher TPA cross section of **2** is attributed to the cumulative effect of the extensive π-delocalization pathway and charge transfer character of the Q-band[7a] caused by the different meso-substituents at the middle and terminal porphyrin units. These are the most desired factors for molecules to exhibit superior nonlinear optical properties by virtue of the large change in dipole moment in their higher excited states. On the other hand, the nonplanar orientation of porphyrin rings in **3** reduces the electronic coupling between the adjacent porphyrin units due to poor p-orbital overlap. As a result, the TPA value does not increase in proportion to the number of constituent chromophores and π-conjugation length.

We have achieved the increased π-electron delocalization efficiency in multiporphyrin arrays by means of improving the coplanarity of porphyrin macrocyles through the formation of supramolecular ladders and prisms with an anticipation to enhance the TPA efficiency. However, an enhancement in TPA cross section in the ladder form is noted only for **2** whereas **1** remains intact because the π-conjugation strength does not change much from single-strand to ladder form. Although the ethyne linkage ensures the coplanarity of the molecule, it tends to deviate from planarity especially in solution in spite of the steric interactions between the closely neighboring β-hydrogens.[23] Hence, the increased TPA cross section value of $\mathbf{2_2Bpy_3}$ is due to elongated π-conjugation length by the restricted free rotation around C−C ethyne linkage which is apparent from the SAXS results and the red-shifted Q-band absorption maximum position of $\mathbf{2_2Bpy_3}$ (ca. 5 nm) with respect to single-strand $\mathbf{2Py_{(excess)}}$. Furthermore, this small change in structure could not account for the observed large enhancement in TPA cross section value of the ladder. Thus there may be a significant contribution to maintain the charge transfer character and cumulenic configuration in the excited state.[24]

Despite the strong enhancement in the extent of π-delocalization of **3** in the duplex form with various ditopic ligands, we have only observed suppressed TPA cross sections with respect to the single-strand (Table 1). Previous studies demonstrate that the TPA efficiency of butadiyne linked linear multiporphyrins is dramatically amplified in the self-assembled duplex form relative to its single-strand and is attributed to the elongated unidirectional π-conjugation length arising from planarization.[10,11] In our cases, however, **3** has a symmetrical star shaped structure with competing two-dimensional π-conjugation pathways along the central porphyrin unit. In fact, multidimensionally branched organic structures are considered

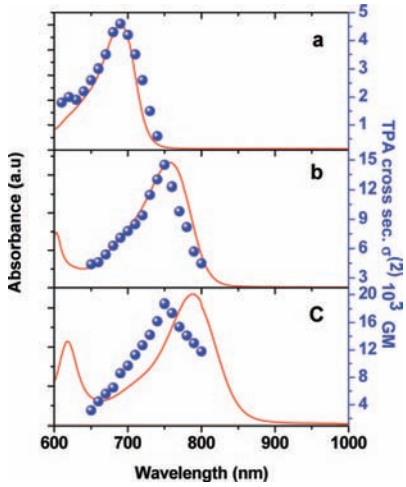

Figure 4. Two-photon (dot) and one photon (solid line) absorption spectrum of (a) dimer **1**, (b) trimer **2** and (c) pentamer **3** in dichloromethane.

to be advantageous, as the intramolecular interaction in branched multichromophores leads to the enhanced TPA cross sections.[2b,25] The reduced TPA value of **3** is probably due to the augmented competitiveness for π-electron delocalization along the mutually perpendicular molecular axes in the rigid and planar duplex form, which diminishes the excited-state transition dipole moment and also destabilizes the excited-state cumulenic configuration. To further strengthen our arguments, we have calculated the frontier molecular orbitals of pentamer **3** without meso-substituents in its coplanar geometry, where the electron density is distributed mostly along the one axis in HOMO level. In addition, the LUMO manifests exclusively unidirectional electron delocalization exhibiting extensive cumulenic character (SI, Scheme S5). Thus it confirms that the increased competition for the excited-state cumulenic configuration and electron density distribution among the porphyrin units in the two perpendicular axes diminishes the TPA efficiency of **3**.

Insight into the role of the self-assembled structure on nonlinear optical properties is gleaned from the TPA studies of multiporphyrinic prisms. The TPA values of **1**and **2** in the prism configuration are drastically decreased with respect to single-strand even though its planarity is comparable to the ladder form (Table 1). Although this observed feature has not been fully understood yet, the shape of the self-assembly, which determines the nature and mode of interstrand interaction between the multiporphyrin units, presumably influences the intrinsic TPA property of the single-strand. Hence, our studies suggest the importance of the shape of the self-assembly in addition to that prism configuration is not suitable for the enhancement of TPA efficiency, although the degree of planarity and π-conjugation efficiency is found to increase similar to ladder form.

The TPA spectra of multiporphyrins **1** and **2** exactly coincide with their one-photon Q-absorption band in concurrence with extended π-electron delocalization strength, as shown in Figure 4. Furthermore, unlike the one-photon absorption spectrum the TPA spectrum remains intact with respect to the zinc coordination environment, again reinforcing the idea that the TPA property of multiporphyrins originates exclusively from its π-conjugation pathway (SI, Figure S10−13). Interestingly, in this case one- and two-photon allowed energy levels are nearly identical or isoenergetic, which contrasts with the previous study on a structurally similar dimer[26] in the Soret regions and suggests that the selection rules for one- and two-photon allowed transitions are mutually exclusive.[27] A recent theoretical investigation by Shai et al.[28] indicates that, even the low-energy two- and one-photon energy levels are alternative and the respective transitions are HOMO−LUMO+3 and HOMO−LUMO. Hence, the key factor is presumably the nature of the B- and Q-band transitions; the one-photon Soret transition is derived mainly from the transition dipole changes, and the Q transition is forbidden in character but gains its intensity through the vibronic coupling from the B-band.[29] Similarly, we assume that there may be a possibility for relaxation of the selection rule for low-energy two-photon transition; as a consequence one- and two-photon transitions are nearly isoenergetic.

In contrast with linear multiporphyrins, the TPA spectrum of **3** (Figure 4c) is blue-shifted with respect to its one-photon Q-band (λ_{max}, Q = 787, TPA = 750 nm). Interestingly, this transition energy is indistinguishable from that of trimer **2**. This feature reflects that two-photon absorption efficiency of pentamer **3** essentially originates from its basic unidirectional trimer unit rather than the overall molecular framework. Because of the steric interaction between the meso-substituents, it is impossible to preserve all constituent porphyrin macrocyles of **3** in coplanar configuration. In parallel with the linear analogues, the TPA maximum position of **3** remains unaltered even after the formation of $\mathbf{3}_2\mathbf{L}_5$ duplex (SI, Figure S12−13). In accordance with the increased π-delocalization length in duplex form, we can expect the red-shifted TPA maximum position compared to single-strand. Nonetheless, this transition is reminiscent of the trimer **2**, pointing out that the TPA property of the pentamer arises exclusively from the trimer unit, which is in good agreement with the observed TPA cross section values. This interpretation is also supported by the molecular orbital pictures of pentamer **3**, where the electron density of the HOMO is distributed mostly along the one axis and the LUMO manifests the unidirectional electron delocalization (SI, Scheme S5).

Conclusions

We have prepared ethyne bridged multiporphyrin ladders and prisms by ligand mediated supramolecular assembly using ditopic and tritopic ligands, respectively. Small- and wide-angle X-ray scattering studies confirm the formation of supramolecular ladder and prism structures. The supramolecular complexation of the pentamer with ditopic ligands enhances the planarity of the molecule and the degree of planarity is sensitive to the molecular length of the ligand. We have shown that the TPA cross sections of multiporphyrins increase nonlinearly by several orders of magnitude with an increase in the number of porphyrin pigments. Such a dramatic enhancement in the TPA cross sections is attributable to the cumulative effect of π-conjugation length, charge transfer character and cumulenic configuration. An attempt to obtain larger TPA cross sections by increasing the number of porphyrin units in the pentamer is mitigated by its nonplanar structure. The TPA study on porphyrinic prisms demonstrates that the overall self-assembled structure and the interstrand interaction between the porphyrin units play an important role in determining their nonlinear optical properties. We have also shown that the elongation of the two-dimensional π-conjugation length in the pentamer destabilizes the cumulenic configuration and consequently reduces the TPA efficiency. The TPA maximum position is mainly determined by the π-delocalization pathway. Furthermore, the coordination environment of central zinc metal does not perturb the two-photon energy levels although it does for one-photon energy levels. We have also demonstrated that the TPA property of the pentamer arises from its basic trimer unit rather than the entire molecule. Finally, on the basis of our investigations, we can emphasize that

although TPA behavior is predicted by the extent of π-conjugation, increasing the degree of π-conjugation at the expense of destabilizing necessary structural features will not yield fruitful results.

Acknowledgment. The work at Yonsei was financially supported by the Star Faculty Program of the Ministry of Education and Human Resources Development of Korea (DK). S.E., Z.S.Y. and J.M.L. thank the fellowship of the BK21 program from the Ministry of Education and Human Resources Development. The work at National Chung Hsing University was financially supported by the National Science Council of Taiwan and in part by the Ministry of Education of Taiwan, under the ATU plan. Research at Northwestern was supported by the Office of Naval Research under grant No. N00014-05-1-0021. Use of the Advanced Photon Source was supported by the U.S. Department of Energy, Office of Science, Office of Basic Energy Sciences, under Contract No. DE-AC02-06CH11357.

Supporting Information Available: UV−visible absorption and fluorescence spectra, spectrophotometric titration spectra, binding constants, schemes, SAXS structures, MO's and TPA spectra of ladders and prisms. This information is available free of charge via the Internet at http://pubs.acs.org.

References and Notes

(1) Lin, T.-C.; Chung, S.-J.; Kim, K.-S.; Wang, X.; He, G. S.; Swaitkiewicz, J.; Pudeavar, H. E.; Prasad, P. N. *Adv. Polym. Sci.* **2003**, *161*, 157.

(2) (a) Reinhardt, B. A.; Brott, L. L.; Clarson, S. J.; Dillard, A. G.; Bhatt, J. C.; Kannan, R.; Yuan, L.; He, G. S.; Prasad, P. N. *Chem. Mater.* **1998**, *10*, 1863. (b) Bhaskar, A.; Guda, R.; Haley, M. M.; Goodson, T., III *J. Am. Chem. Soc.* **2006**, *128*, 13972.

(3) Albota, M.; Beljonne, D.; Bredas, J.-L.; Ehrlich, J. E.; Fu, J.-Y.; Heikal, A. A.; Hess, S. E.; Kogej, T.; Levin, M. D.; Marder, S. R.; McCord-Maughon, D.; Perry, J. W.; Rockel, H.; Rumi, M.; Subramaniam, G.; Webb, W. W.; Wu, X.-L.; Xu, C. *Science* **1998**, *281*, 1653.

(4) Karotki, A.; Drobizhev, M.; Kruk, M.; Spangler, C.; Nickel, E.; Mamardashivili, N.; Rebane, A. *J. Opt. Soc. Am. B* **2003**, *20*, 321.

(5) (a) Kadishi, K. M. ; Smith, K. M.; Guilard, R. *The Porphyrin Handbook*; Academic Press: Oxford, U.K., 2003; *Vols. 1−20*. (b) Kim, K. S.; Noh, S. B.; Katsuda, T.; Ito, S.; Osuka, A.; Kim, D. *Chem. Commun.* **2007**, *2479*. (c) Yoon, M.-C.; Noh, S. B.; Tsuda, A.; Nakamura, Y.; Osuka, A.; Kim, D. *J. Am. Chem. Soc.* **2007**, *129*, 10080. (d) Rath, H.; Sankar, J.; PrabhuRaja, V.; Chandrashekar, T. K.; Nag, A.; Goswami, D. *J. Am. Chem. Soc.* **2005**, *127*, 11608. (e) Rath, H.; Prabhuraja, V.; Chandrashekar, T. K.; Nag, A.; Goswami, D.; Joshi, B. S. *Org. Lett.* **2006**, *8*, 2325. (f) Misra, R.; Kumar, R.; Chandrashekar, T. K.; Nag, A.; Goswami, D. *Org. Lett.* **2006**, *8*, 629. (g) Yoon, Z. S.; Kwon, J. H.; Yoon, M.-C.; Koh, M. K.; Noh, S. B.; Sessler, J. L.; Lee, J. T.; Seidel, D.; Aguilar, A.; Shimizu, S.; Suzuki, M.; Osuka, A.; Kim, D. *J. Am. Chem. Soc.* **2006**, *128*, 14128.

(6) Ahn, T. K.; Kim, K. S.; Kim, D. Y.; Noh, S. B.; Aratani, N.; Ikeda, C.; Osuka, A.; Kim, D. *J. Am. Chem. Soc.* **2006**, *128*, 1700.

(7) (a) Lin, V. S.-Y.; DiMagno, S. G.; Therien, M. J. *Science* **1994**, *264*, 1105. (b) Duncan, T. V.; Susumu, K.; Sinks, L. E.; Therien, M. J. *J. Am. Chem. Soc.* **2006**, *128*, 9000. (c) Anderson, H. L. *Chem. Commun.* **1999**, 2323.

(8) Hisaki, I.; Hiroto, S.; Kim, K. S.; Noh, S. B.; Kim, D.; Shinokubo, H.; Osuka, A. *Angew. Chem.* **2007**, *46*, 5125.

(9) Pfeil, A.; Lehn, J. M. *J. Chem, Soc., Chem. Commun.* **1992**, 838.

(10) (a) Anderson, H. L. *Inorg. Chem.* **1994**, *33*, 972. (b) Drobizhev, M.; Stepanenko, Y.; Rebane, A.; Wilson, C. J.; Screen, T. E. O.; Anderson, H. L. *J. Am. Chem. Soc.* **2006**, *128*, 12432.

(11) (a) Dy, J. T.; Ogawa, K.; Satake, A.; Ishizumi, A.; Kobuke, Y. *Chem. Eur. J.* **2007**, *13*, 3491. (b) Ogawa, K.; Ohashi, A.; Kobuke, Y.; Kamada, K.; Ohta, K. *J. Am. Chem. Soc.* **2003**, *125*, 13356. (c) Ogawa, K.; Ohashi, A.; Kobuke, Y.; Kamada, K.; Ohta, K. *J. Phys. Chem. B* **2005**, *109*, 22003.

(12) Lee, S. J.; Mulfort, K. L.; O′Donnell, J. L.; Zuo, X.; Goshe, A. J.; Wesson, P. J.; Nguyen, S. T.; Hupp, J. T.; Tiede, D. M. *Chem. Commun.* **2006**, 4581.

(13) (a) Huang, T. H.; Chen, Y-J.; Lo, S-S.; Yen, W-N.; Mai, C-L.; Kuo, M-C.; Yeh, C-Y. *Dalton Trans.* **2006**, 2207. (b) Lin, V. S.-Y.; Therien, M. J. *Chem. Eur. J.* **1995**, *1*, 645.

(14) Mongin, O.; Papamicaël, C.; Hoyler, N.; Gossauer, A. *J. Org. Chem.* **1998**, *63*, 5568.

(15) Seifert, S.; Winans, R. E.; Tiede, D. M.; Thiyagarajan, P. *J. Appl. Crystallogr.* **2002**, *33*, 782.

(16) *Hyperchem*, version 5.02; Hypercube, Inc.: Gainesville, FL, 1997.

(17) Zhang, R.; Thiyagarajan, P.; Tiede, D. M. *J. Appl. Crystallogr.* **2000**, *33*, 565.

(18) *Specfit*, version 3; Spectrum Software Associates, P.O. Box 4494, Chapel Hill, NC 27515−4494.

(19) Screen, T. E. O.; Throne, J. R. G.; Denning, R. G.; Bucknall, D. G.; Anderson, H. L. *J. Am. Chem. Soc.* **2002**, *124*, 9712.

(20) Glatter, O. *Neutron, X-ray and Light Scattering*; Elsevier: Amsterdam, 1991. Guinier, A.; Fournet, G. *Small Angle Scattering of X-rays*;Wiley: New York, 1955.

(21) Svergun, D. I. *J. Appl. Crystallogr.* **1992**, *25*, 495.

(22) (a) Hunter, C. A.; Sanders, J. K. M.; Stone, A. *J. Chem. Phys.* **1989**, *133*, 395. (b) Hunter, C. A.; Meah, M. N.; Sanders, J. K. M. *J. Am. Chem. Soc.* **1990**, *112*, 5773. (c) Mak, C. C.; Bampos, N.; Sanders, J. K. M. *Angew. Chem. Int. Ed. Engl.* **1998**, *37*, 3020. (d) Mak, C. C.; Pomeranc, D.; Montalti, M.; Prodi, L.; Sanders, J. K. M. *Chem. Commun.* **1999**, 1083.

(23) (a) Rubtsov, I. V.; Susumu, K.; Rubtsov, G. I.; Therien, M. J. *J. Am. Chem. Soc.* **2003**, *125*, 2687. (b) Kumble, R.; Palese, S.; Lin, V. S.-Y.; Therien, M. J.; Hochstrasser, R. M. *J. Am. Chem. Soc.* **1998**, *120*, 11489.

(24) Kninek, I.; Klimovic, J.; Prasad, P. N. *Chem. Mater.* **1993**, *5*, 357.

(25) (a) Wang, Y.; He, G. S.; Prasad, P. N.; Goodson, T., III *J. Am. Chem. Soc.* **2005**, *127*, 10128. (b) Goodson, T., III *Acc. Chem. Res.* **2005**, *38*, 99.

(26) (a) Drobizhev, M.; Stepanenko, Y.; Dzenis, Y.; Karotki, A.; Rebane, A.; Taylor, P. N.; Anderson, H. L. *J. Am. Chem. Soc.* **2004**, *126*, 15352. (b) Drobizhev, M.; Stepanenko, Y.; Dzenis, Y.; Karotki, A.; Rebane, A.; Taylor, P. N.; Anderson, H. L. *J. Phys. Chem. B* **2005**, *109*, 7223.

(27) (a) Drobizhev, M.; Karotki, A.; Kruk, M.; Rebane, A. *Chem. Phys. Lett.* **2002**, *355*, 175. (b) Karotki, A.; Drobizhev, M.; Dzeins, Y.; Taylor, P. N.; Anderson, H. L.; Rebane, A. *Phys. Chem. Chem. Phys.* **2004**, *6*, 7.

(28) Zhu, L.; Yi, Y.; Shuai, Z.; Schmidt, K.; Zojer, E. J. *Phys. Chem. B* **2007**, *111*, 8509.

(29) Kalyansundaram, K. *Photochemistry of polypyridine and porphyrin complexes*; Academic Press: New York, 1992; p 401.

JP801626S